

Theoretical study of the atomic structure of silicon (211), (311), and (331) surfaces

D. J. Chadi

Xerox Palo Alto Research Center, 3333 Coyote Hill Road, Palo Alto, California 94304

(Received 5 July 1983)

The structural and energetic aspects of high-Miller-index Si surfaces were investigated by studying the (211), (311), and (331) vicinal surfaces. Several types of new structural models for (211) and (311) surfaces were examined. For (211) and especially (311) surfaces, dangling-bond densities appreciably lower than on the (111) surface can be obtained. The calculated surface energies of the ideal and reconstructed vicinal surfaces were, however, in all cases higher than that of the Si(111)- 2×1 π -bonded chain structure.

I. INTRODUCTION

High-Miller-index surfaces, even though less extensively studied than the (100), (110), and (111) surfaces, are interesting for several reasons. First, they exhibit combinations of bonding configurations which do not normally occur simultaneously on any given low-Miller-index surface. The greater complexity of these surfaces is sometimes useful. For example, the "ideal" (311) surface has equal densities of threefold- and twofold-coordinated surface atoms. It can be viewed to be an average, in some sense, of the (100) and (111) surfaces. The (311) surface has several desirable properties that are absent on the (111) and (100) surfaces. In a III-V material, such as GaAs, the (311) surface would be nonpolar, in contrast with the other two surfaces. Superior crystal-growth properties have been observed on the (311) surface rather than on the (100), (111), or on nonpolar (110) surfaces.^{1,2} Similarly, the Si(211) surface has been used for epitaxial growth of GaP-Si interfaces to improve its electronic properties in comparison with interfaces grown on other surfaces.³ The study of the high-Miller-index surfaces is interesting also from the structural stability viewpoint. The questions of whether such surfaces can lead to lower surface energies than can be realized on a low-Miller-index surface⁴ and of phase transitions between different structures are important.^{5,6}

In this paper the results of theoretical investigations of (211), (311), and (331) surfaces are reported. In Sec. II the structural aspects of vicinal surfaces, resulting from step formation on (111) surfaces, are discussed. Results of surface-energy calculations on (211), (311), and (331) surfaces are presented in Secs. III-V. The tight-binding approach used in the calculations is examined in Sec. VI.

II. GEOMETRICAL ASPECTS OF STEPPED (111) SURFACES

A. Steps propagating along the $[\bar{1}\bar{1}2]$ direction

The top view of the Si(111) surface is shown in Fig. 1(a). By taking the cubic $[\bar{1}10]$, $[\bar{1}\bar{1}2]$, and $[111]$ directions shown in Fig. 1(b) to be along the x , y , and z directions of the surface coordinate system, the lattice vectors

$\vec{R}_{\pm} = (R_x, \pm R_y, R_z)$ of the 1×1 surface are given by

$$\vec{R}_{\pm} = (\frac{1}{2}, \pm\sqrt{3}/2, 0) \tag{1}$$

in units of the surface hexagonal lattice constant.

Any periodic step array propagating along the cubic $[\bar{1}\bar{1}2]$ direction (e.g., see Fig. 2) with only one double layer of atoms removed in going from one terrace to the next is described by the translation vectors

$$\vec{R}_1 = (1, 0, 0), \tag{2}$$

$$\vec{R}_2 = (0.5\delta_p, (1.5p + 1)/\sqrt{3}, -2/\sqrt{6}), \quad p = 0, 1, 2, \dots \tag{3}$$

where

$$\delta_p = \begin{cases} 1 & p = \text{odd integer} \\ 0 & \text{otherwise} \end{cases} \tag{4}$$

The periodically stepped surfaces for different values of p in Eq. (2) can be considered to be vicinal surfaces which can be identified by the directions of the surface normal

$$\vec{n} = (p + 2, p, p). \tag{5}$$

The angle of inclination θ of these surfaces relative to the (111) surface can be obtained from the relation

$$\tan\theta = \frac{\sqrt{2}}{(1.5p + 1)}. \tag{6}$$

The $(\bar{1}\bar{1}2)$ propagating surfaces are inclined from the

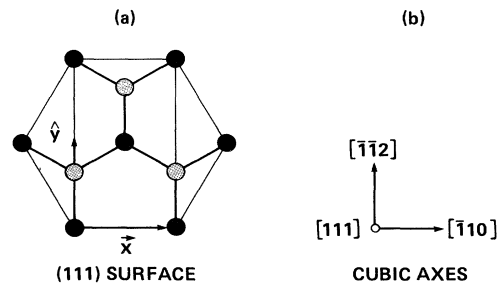


FIG. 1. Top view of the Si(111) surface is shown in (a). Solid and dashed circles represent surface and second-layer atoms, respectively. The relation of the surface coordinate system to the bulk cubic axes is shown in (b).

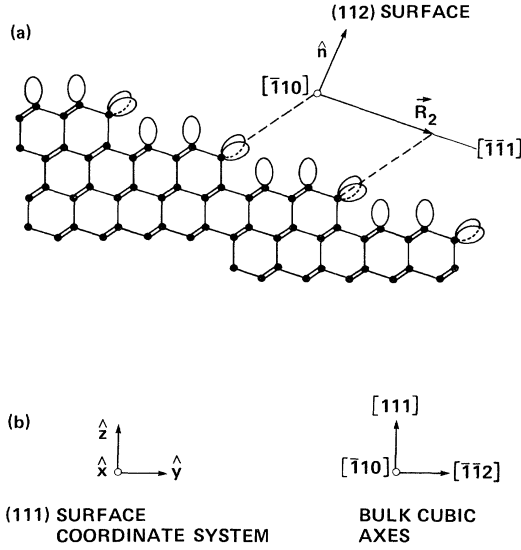


FIG. 2. Side view of the ideal Si(111) surface. The surface unit cell contains two threefold-coordinated terrace atoms and twofold-coordinated step atom. The coordinate axes are shown relative to the bulk cubic axes.

(111) surface toward the (100) surface. The inclination is largest for small values of p . The surface normals⁷ and tilt angles for several values of p are

$$p = 0, \quad \vec{n} = (1, 0, 0), \quad \theta = 54.74^\circ, \quad (7)$$

$$p = 1, \quad \vec{n} = (3, 1, 1), \quad \theta = 29.50^\circ, \quad (8)$$

$$p = 2, \quad \vec{n} = (2, 1, 1), \quad \theta = 19.47^\circ, \quad (9)$$

$$p = 3, \quad \vec{n} = (5, 3, 3), \quad \theta = 14.42^\circ. \quad (10)$$

These four surfaces have been seen in low-energy electron diffraction (LEED) measurements.⁵ All show reconstructions and order-disorder transitions at elevated temperatures. For the *ideal structures* considered in this section the “terrace” atoms are threefold coordinated and the “step” atoms are twofold coordinated. The number of terrace atoms n_{terrace} per unit which is an indicator of terrace width is simply given by

$$n_{\text{terrace}} = p. \quad (11)$$

The ideal (100) surface which corresponds to $p = 0$ in Eq. (7) has no terrace (i.e., threefold-coordinated) atoms. The ideal (311) surface has one terrace and one step atom per unit cell. In a III-V material the two atoms are of opposite type. The reconstructions of the (311) and (211) surfaces are examined in the following two sections. The reconstructions lead to a decrease in the density of dangling bonds in most cases.

The steps seen in LEED are not always of a double-layer height. The general expression for the translation vectors of an unreconstructed periodic step array having m double layers missing between terrace atoms is given by⁸

$$\vec{R}_1 = (1, 0, 0), \quad (12)$$

$$\vec{R}_2 = (0.5\delta_p, (1.5p + m)/\sqrt{3}, -2m/\sqrt{6}). \quad (13)$$

The surface normals are given by

$$\vec{n} = (p + 2m, p, p) \quad (14)$$

and the angle of inclination with respect to the (111) surface is

$$\tan\theta = \frac{m\sqrt{2}}{(1.5p + m)}, \quad (15)$$

which for $m = 1$ reduce to Eqs. (4) and (5), respectively. The (511) and (711) surfaces seen⁵ in LEED correspond to multilayer steps with

$$p = 1, \quad m = 2, \quad \vec{n} = (5, 1, 1), \quad \theta = 38.94^\circ, \quad (16)$$

$$p = 1, \quad m = 3, \quad \vec{n} = (7, 1, 1), \quad \theta = 43.31^\circ. \quad (17)$$

The value of n_{terrace} for the surfaces defined by Eqs. (13) and (14) is still correctly given by Eq. (11). The number of step (i.e., twofold sites) sites n_{step} per ideal unit cell is given by

$$n_{\text{step}} = m, \quad (18)$$

where m specifies the number of double layers missing between two adjacent terraces.

Equations (13) and (14) show that when m and p are both multiplied by a constant integer q , which physically corresponds to a simultaneous increase of terrace widths and heights by a factor of q , the surface normal does not change direction. For example, for $m = 1$ (i.e., one double layer missing between terraces) and for $p = 2$, we get a (211) surface. Similarly, for $m = 2$ and $p = 4$, we again find a (211) surface. The two surfaces, however, are quite different in atomic structure even though they have the same inclination to the [111] axis. By measuring the splitting of the primary order LEED spots, it is possible to distinguish between the two surfaces.^{5,9} The (211) surface seen experimentally is found to correspond to the first case. Interesting reversible order-order transitions (at $T \simeq 800^\circ\text{C}$) have been reported to occur between the two types of surfaces.^{5,6}

B. Steps propagating along the $[1\bar{1}\bar{2}]$ direction

Steps along the $[\bar{1}\bar{1}\bar{2}]$ direction discussed above are characterized by threefold-coordinated (111)-like and twofold-coordinated (100)-like terrace and step atoms, respectively, in the ideal geometry. Steps propagating along the $[11\bar{2}]$ direction (Fig. 3) are characterized by threefold-coordinated terrace and step atoms. For an ideal structure, the general expression for the primitive translation vectors for a periodic 1×1 step having m double layers missing between neighboring terraces is given by⁸

$$\vec{R}_1 = (1, 0, 0), \quad (19)$$

$$\vec{R}_2 = \left[0.5\delta_{p+m}, -\frac{(1.5p + 0.5m)}{\sqrt{3}}, -2m/\sqrt{6} \right], \quad (20)$$

where δ is defined by Eq. (4).

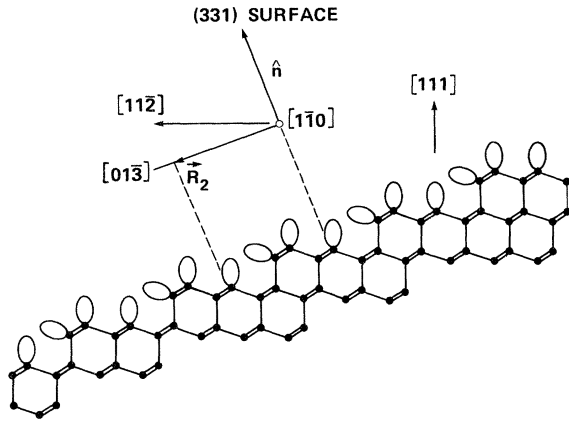


FIG. 3. Side view of the ideal Si(331) surface resulting from step propagation along the $[11\bar{2}]$ direction of the (111) surface.

The surface normal (relative to the bulk cubic axes) is given by

$$\vec{n} = (p + m, p + m, p - m), \quad p \geq m \geq 1 \quad (21)$$

and its inclination away from the $[111]$ axis is obtained from

$$\tan \theta = \frac{2m\sqrt{2}}{3p + m} \quad (22)$$

For $m = 1$, corresponding to steps of one double-layer height, the surface normals and tilt angles for some values of p are

$$p = 1, \quad \vec{n} = (1, 1, 0), \quad \theta = 35.26^\circ, \quad (23)$$

$$p = 2, \quad \vec{n} = (3, 3, 1), \quad \theta = 22.00^\circ, \quad (24)$$

$$p = 3, \quad \vec{n} = (2, 2, 1), \quad \theta = 15.79^\circ. \quad (25)$$

The total number of dangling bonds per unit cell is $p + 1$ for each structure.

III. (211) SURFACES

The "ideal" (211) surface resulting from cleavage at an angle of $\approx 19.5^\circ$ from the $[111]$ axis is shown in Fig. 2(a). The unit cell of the 1×1 surface contains two threefold-coordinated terrace atoms and one twofold-coordinated step (or edge) atom. For this structure the edge atoms are expected to dimerize leading to a doubling of the lattice vector along the x (i.e., the cubic $[\bar{1}10]$) direction. We have previously examined the atomic and electronic structure of the dimerized (211)- 2×1 surface.¹⁰ At the time only buckling distortions of the two terrace atoms were examined. In the present study the calculations were extended to π -bonded chain-type reconstructions of the terrace atoms similar to that occurring on the Si(111)- 2×1 surface.^{11,12} The small width of the terrace is found to strongly inhibit this type of reconstruction. Since recent theoretical studies indicate that a buckling distortion is also not energetically favorable,^{11,12} one must conclude that the terrace atoms are essentially in their ideal positions in the absence of other identifiable relaxation mecha-

nisms. This would be consistent with indirect experimental evidence^{13,14} for the presence of 1×1 regions at terrace atoms near a step.

As far as the relaxation of step atoms is concerned, the issue of dimerization along the $[\bar{1}10]$ axis has been controversial. Evidence for 2×1 reconstruction along the edge is seen in some LEED studies^{5,6} but not in others.¹⁵ Olshansky *et al.* find temperature-induced order-disorder transitions at the surface. Kaplan¹⁵ finds no evidence for a reconstruction along the edge atoms. Pandey has recently suggested a model that, when applied to the (211) surface, would explain this result.⁴ The model is created by separating the two halves of a crystal along the dotted line shown in Fig. 4(a). Rebonding of terrace atoms as shown in Fig. 4(b) leads to a structure that is very stable against reconstruction along the $[\bar{1}10]$ direction. In addition, the dangling-bond density is appreciably reduced. By denoting the dangling-bond density on the ideal Si(111)- 1×1 surface by n_0 with

$$n_0 = 2/(\sqrt{3}a^2) \quad (26)$$

(where a is the hexagonal lattice constant), the corresponding dangling-bond density n for the (211) surface in Fig. 4 is only $\approx 71\%$ of n_0 ; in fact

$$n_{211} = n_{111}/\sqrt{2}. \quad (27)$$

The large drop in the dangling-bond density has raised the question⁴ of whether the (111) surface, ideal or reconstructed, is stable against surfaces such as the (211). On the basis of simple bond counting and strain energy argu-

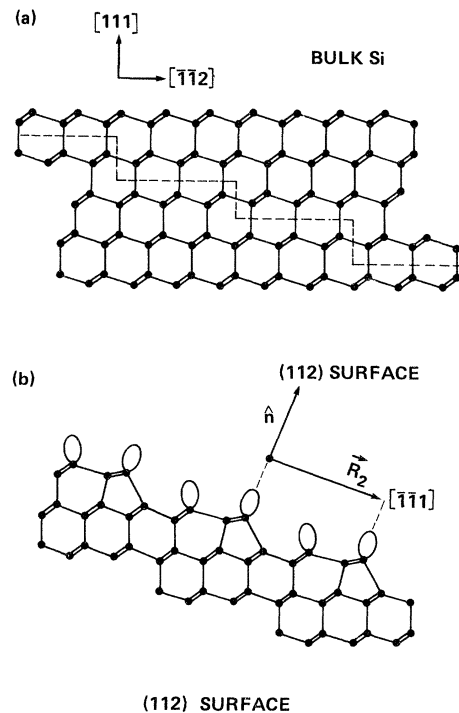


FIG. 4. Side view of the Si(111) surface is shown in (a). The dashed line passes through bonds broken in the process of forming a (112) surface with a low dangling-bond density. The atomic relaxations occurring after cleavage are shown in (b).

ments, Pandey has suggested⁴ that the (111) surface is in fact unstable with respect to the reconstructed high-Miller-index surfaces. Our total-energy calculations for the (111)- 2×1 π -bonded chain structure and for ideal and relaxed (211) surfaces show that the surface energy of the (111) surface is appreciably lower than that of the (211) surface despite the fact that the latter has a significantly lower dangling-bond density. The surface energy is calculated to be¹⁶

$$\gamma_{211} = 1.2 \quad (28)$$

(eV/unit area) for the (211) surface as compared to a value of 1.06 ± 0.06 eV/unit area for the (111)- 1×1 surface.¹⁷ The primary reason for the larger value of γ_{211} is that the bonding in Fig. 4(b) cannot be achieved without substantial bondlength as well as angular strains. The energy-minimized structure is found to have bondlength expansions as large as 5.7%. The lower surface energy of the (111) surface compared to the (211) surface is consistent with experiment.

The surface energy of the (211)- 2×1 surface which has twofold-coordinated step atoms in the ideal structure and dimerized atoms in the reconstructed geometry was also calculated and found to be¹⁶

$$\gamma_{211} = 1.4 \quad (29)$$

(eV/unit area) for the latter. The small 0.2-eV difference between the values of the surface energy for the two different (211) structures suggests that either geometry could occur at the surface depending on surface preparation. This would explain the observation of twofold and fourfold periodicities along the $[\bar{1}10]$ direction in one set of LEED experiments^{5,6} (indicative of dimerization) and not in the other.¹⁵ The geometry of the (211) surface is an important consideration in epitaxial growth of polar surfaces on nonpolar surfaces.³ The arguments of Wright *et al.*³ suggest that optimal interface properties are expected for the higher dangling-bond density (211) surface.

IV. (311) SURFACE

The ideal (311) surface is unique among the vicinal surfaces of Si in that it contains equal numbers of step and terrace atoms; in fact, there are just two atoms per unit cell which are twofold and threefold coordinated, respectively, as shown in Fig. 5. On a III-V material, such as GaAs, there are two (311) surfaces which differ only by an interchange of all Ga and As atoms. The two surfaces have Ga and As surface atoms at twofold- and threefold-coordinated sites, respectively, or vice versa. As mentioned above, very good III-V crystal-growth properties on (311) surfaces have been observed.^{1,2} The neutrality of these surfaces together with the very different atomic coordination of the surface atoms may provide an ideal solution to the dual problems of charge neutrality and site selectivity³ for epitaxial growth of polar-nonpolar interfaces.

The translation vectors of the (311)- 1×1 surface with respect to the coordinate axes [shown in Fig. 1(a)] are⁸

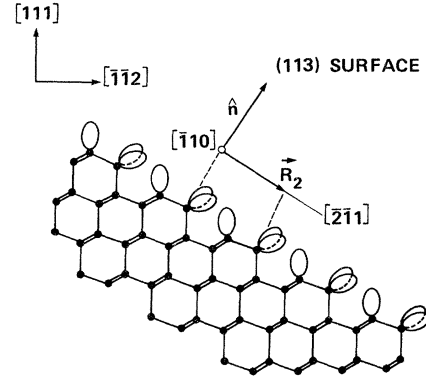


FIG. 5. Side view of the ideal Si(113) surface. The unit cell contains one threefold- and one twofold-coordinated atom.

$$\vec{R}_1 = (1, 0, 0), \quad (30)$$

$$\vec{R}_2 = \left(\frac{1}{2}, 2.5/\sqrt{3}, -2/\sqrt{6}\right). \quad (31)$$

The orientation of these vectors with respect to the bulk cubic axes is shown in Fig. 5. The Si(311) surface is 3×2 reconstructed.⁵ The reconstructed surface has a threefold periodicity along \vec{R}_1 (i.e., along the cubic $[\bar{1}10]$ direction) and a twofold periodicity along \vec{R}_2 . The threefold periodicity along \vec{R}_1 also occurs for the (511) surface.

The reconstruction of the (311) surface was examined by taking slab geometries with 1×1 , 3×1 , and 3×2 periodicities with up to 120 atoms per unit cell. Dimer, trimer, and a reconstruction leading to a large decrease in the surface dangling-bond density [similar to that discussed for the (211) surface] were examined. The total energy and surface energy per unit area was calculated in each case for comparison with other Si surfaces. A description of the surface structures and the results of the calculations for Si are described below.

The relaxation and/or reconstruction of the (311) surface can lead to an extremely low dangling-bond density. The rebonding mechanism at steps, suggested by Pandey⁴ and shown in Figs. 4(a) and 4(b) for the case of the (211) surface, when applied to the (311) surface leads to a dangling-bond density only 52% of that on the ideal Si(111)- 1×1 surface. This rebonding leads to a onefold periodicity along \vec{R}_1 in disagreement with the threefold periodicity seen experimentally.⁵ The structure is interesting nonetheless for studying the energy-structural aspects of surface reconstruction. The ultralow dangling-bond density (311) surface is calculated to have a surface energy¹⁶ of

$$\gamma_{311} = 1.66 \quad (32)$$

(eV/unit area), which is appreciably higher than the corresponding figure for the (211) surface or, in fact, for the ideal Si(111)- 1×1 for which¹⁷

$$\gamma_{111} = 1.06 \pm 0.06 \quad (33)$$

(eV/unit area). The energy-minimized (311) structure shows both large bond-length ($\approx 6\%$) and angular strains. To check whether the small size of the unit cell was re-

sponsible for the large surface energy, the calculations (for the Pandey-type reconstruction) were also performed for 3×1 and 3×2 cells using slab geometries with up to 120 atoms. The surface energy for the 3×1 cell (where the periodicity is threefold along \vec{R}_1) was found, as might be expected, to be the same as for the 1×1 surface. For the 3×2 surface a surface energy¹⁶

$$\gamma_{311} = 1.53 \quad (34)$$

(eV/unit area), which is not significantly lower than that for the (311)- 1×1 surface was calculated. These results indicate that this type of dangling-bond reducing reconstruction considered here is very unlikely to explain the Si(311) surface structure.

A completely different type of reconstruction involving trimerization along \vec{R}_1 (i.e., along the cubic $[\bar{1}10]$ direction) was also tested. This reconstruction inherently leads to a threefold periodicity along \vec{R}_1 . For the trimer structures

$$\gamma_{311} = 1.37 \quad (35)$$

(eV/unit area) is also large as the result of large strains.¹⁶

V. (331) SURFACE

A side view of the ideal (331) surface is shown in Fig. 3. As can be seen, the surface can be obtained as a result of steps propagating along the $[11\bar{2}]$ direction of the (111) surface. Periodic arrays of such steps are formed upon laser annealing after cutting the Si(111) surface along the $[11\bar{2}]$ direction.¹⁸ Steps of single- or double-layer height are seen,^{6,18} similar to the case for $(\bar{1}\bar{1}2)$ steps.^{5,19}

Steps propagating along the $[11\bar{2}]$ direction do not result from cleavage.⁹ Our calculations show that this does not occur as a result of a higher surface energy for these steps. In particular, the surface energy

$$\gamma_{311} = 1.09 \quad (36)$$

(eV/unit area) for the relaxed (331)- 1×1 surface is found to be lower than γ_{211} . The tendency of the surface not to form (331)-type steps during cleavage is, therefore, not related to a high surface energy but is connected with the reconstruction of the Si(111)- 2×1 surface in the process of cleavage. The occurrence of the π -bonded chain structure during cleavage requires surface atomic displacements along the $[\bar{1}\bar{1}2]$ direction. This and the very small activation barrier in going from the 1×1 to the 2×1 chain structure together with the small surface energy¹⁶

$$\gamma_{111} = 0.7 \quad (37)$$

(eV/unit area) for the latter geometry is what causes steps to propagate along the $[\bar{1}\bar{1}2]$ direction while suppressing $(11\bar{2})$ -type steps during cleavage. On annealed surfaces, both types of steps are, in fact, observed in vacuum tunneling microscopy experiments. The LEED pattern of the annealed Si(331) surface indicates a 13×1 reconstruction with the translation vector along the $[\bar{1}10]$ direction becoming very large.⁵

VI. METHOD OF CALCULATION

A. Comments on the tight-binding method

The use of the empirical tight-binding method in total-energy calculations has been previously discussed.^{20,21} The method was originally designed to give information on the variation of the total energy as a function of atomic displacements that did not lead to any change in the total number of bonds in the system. Studies of rotational-relaxation models²⁰ for GaAs(110) and of the energy difference between symmetric and asymmetric dimers on the Si(100) surface²¹ were made using this method. The method was later extended in a very simple manner to deal with situations involving changes in the number of bonds within the system. In this way, the change in energy in going from the ideal (100)- 1×1 surface to the dimerized 2×1 surface could also be calculated. These ideas are discussed below.

The nearest-neighbor tight-binding model used in the calculations on Si is specified by the following parameters²¹ (in eV):

$$V_{ss\sigma} = -1.938, \quad V_{sp\sigma} = 1.745, \quad (38)$$

$$V_{pp\sigma} = 3.050, \quad V_{pp\pi} = -1.075, \quad (39)$$

and with "atomic" s and p energies equal to

$$E_s = -5.25, \quad E_p = 1.20. \quad (40)$$

This choice of E_s and E_p sets the zero of energy at the bulk valence-band maximum. The parameters provide a reasonable description of the bulk occupied bands and an approximate description of the conduction bands. The valence-conduction band gap is indirect (≈ 1.14 eV) and is $\Gamma \rightarrow L$ instead of $\Gamma \rightarrow X$ in character.

The variation of the total energy with atomic displacements was originally expressed as²⁰

$$\Delta E_{\text{tot}} = \sum_{\vec{k}} \Delta E_n(\vec{k}) + \sum_i (U_1 \epsilon_i + U_2 \epsilon_i^2), \quad (41)$$

where the sum in the first term is over occupied one-electron states, and where the second term represents a semiempirical correction for the double counting of electron-electron interactions in the first term and includes the ion-ion interaction energy. The subscript i in Eq. (41) denotes a bond, and ϵ_i denotes the fractional change in bond length from its reference value in bulk Si. The two empirical "spring" constants U_1 and U_2 , therefore, have the units of energy. From a fitting to bulk elastic moduli and phonon frequencies the values (in eV)

$$U_1 = -16.36$$

and

$$U_2 = 55.60 \quad (42)$$

were obtained.²¹ In determining U_1 and U_2 , the tight-binding interaction parameters in Eqs. (39) and (40) were assumed to have a d^{-2} dependence on nearest-neighbor distance d . In practice this approximation gives reasonable results for the total energy because of the presence of

the semiempirical terms ($U_1\epsilon + U_2\epsilon^2$) in Eq. (41).

An implicit assumption in writing Eq. (41) is that the atomic displacements do not lead to a change in the number of bonds in the system. This condition does not cause any problem for many systems of interest; however, in comparing surface energies for structures having different numbers of bonds or when calculating bond-breaking energies, it becomes necessary to modify Eq. (41). This can be done in a very simple way, as shown by Vanderbilt and Joannopoulos,²² by adding a term of the form U_0N_{bonds} to the expression for the total energy, where N_{bonds} is the number of bonds in the unit cell and U_0 is a parameter that can be determined from the cohesive energy of the solid. The term U_0N_{bonds} represents essentially the repulsive ion-ion interaction. The variation of this repulsive term with atomic displacements is included in Eq. (40) for situations in which the number of bonds is conserved. The expression

$$\Delta E_{\text{tot}} = \sum_{\vec{k}} \Delta E_n(\vec{k}) + \sum_i (U_1\epsilon_i + 2\epsilon_i^2) + \Delta(U_0N_{\text{bonds}}) \quad (43)$$

generalizes Eq. (41) to situations where bond breaking or bond formation takes place as a result of the atomic motions. The value of U_0 in Si is calculated to be (in eV)

$$U_0 = 4.1. \quad (44)$$

This value is obtained from the cohesive energy, i.e., from the change in total energy in going from the free atom to a bulk atom. The necessity of the last term in Eq. (43) is seen from the fact that in its absence the electronic energy (and, therefore, the total energy) would decrease monotonically with increasing atomic coordination. The inclusion of $\Delta(U_0N_{\text{bonds}})$ makes the occurrence of fivefold-coordinated Si atoms less energetically favorable, in most situations, than the optimal fourfold-tetrahedral coordination.

The expansion in the fractional bondlength change ϵ in Eq. (43) can be carried out to higher orders than ϵ^2 if desired. For the purposes of most calculations the higher-order terms make a negligible contribution to the total energy because $\epsilon \leq 0.1$ in nearly all cases (one important exception is C). For Si the coefficient U_3 of ϵ^3 was estimated, from comparisons of the total-energy variation to results of other calculations, to be approximately -166 eV.

The last component of the total energy missing from Eq. (43) is the Coulombic part. The intra-atomic Coulomb energy for placing two electrons in a dangling-bond orbital and the Madelung energy are, in situations involving large charge transfers, important in determining the nature of the surface reconstruction. For Si, the Hubbard-type repulsive intra-atomic Coulomb energy U_C for placing two electrons in a dangling bond is²³

$$U_C \simeq 1.15 \quad (45)$$

(in eV). The inclusion of this term in the total energy makes surface geometries accompanied by large charge transfers less favorable energetically. Significant charge redistributions can occur primarily on surfaces in which the hopping matrix elements are small. (111)-type surfaces, on which the dangling bonds interact via weak second-neighbor interactions (i.e., $V \simeq 0.1$ eV, $V/U_C \ll 1$), instead of strong first-neighbor interactions ($V \simeq 1-3$ eV, $V/U_C \geq 1$), represent important cases in which the inclusion of the Coulombic terms are essential for obtaining the correct atomic geometry.

The energy term U_C is also important in comparing the energies of ideal and dimerized (100) surfaces. Denoting the two sp^3 dangling-bond orbitals on a given atom on the ideal surface by φ_1 and φ_2 , respectively, we can construct two new orbitals ψ_1 and ψ_2 :

$$\psi_1 = (\varphi_1 + \varphi_2)/\sqrt{2} \quad (46)$$

and

$$\psi_2 = (\varphi_1 - \varphi_2)/\sqrt{2}. \quad (47)$$

The wave functions ψ_1 and ψ_2 are sp and p in character, respectively. The energy reduction in putting an electron in ψ_1 instead of in φ_1 is

$$\Delta E = \frac{E_s + E_p}{2} - \frac{E_s + 3E_p}{4} \quad (48)$$

or

$$\Delta E = \frac{E_s - E_p}{4}, \quad (49)$$

where E_s and E_p are the energies of the atomic s and p orbitals. From Eq. (49) the change in energy from rehybridization is large and is about -1.6 eV. By placing both dangling-bond electrons with opposite spins into ψ_1 the gain in energy will be (in eV)

$$\Delta E = \frac{E_s - E_p}{2} + U_C = -3.2 + 1.15 \quad (50)$$

or

$$\Delta E \simeq -2. \quad (51)$$

In calculations where U_C is neglected, the energy of the (100)- 1×1 surface comes out lower by the amount U_C per unit cell. The energy reduction resulting from dimerization, in going from the 1×1 to a 2×1 surface is, therefore, underestimated by U_C . The dimer bond strength in Si, for $U_C = 0$, was calculated¹⁰ to be approximately 0.67 eV when compared to a 1.82-eV value for²⁴ $U_C = 1.15$ eV. The latter is much closer to the typical bond strength in crystalline Si of 2.35 eV, and to the 1.5-eV result of *ab initio* self-consistent pseudopotential calculations.²⁵

B. Surface energy

The comparison of different surface geometries for the purpose of finding the lowest-energy atomic configuration is facilitated by considering the surface energy per unit area γ . For a system containing N atoms and total energy $E_{\text{tot}}(N)$ the surface energy E_{surf} is defined here as the

difference between $E_{\text{tot}}(N)$ and NE_0 where E_0 is the total energy per atom in the crystalline (diamond-structure) solid:

$$E_{\text{surf}} = E_{\text{tot}}(N) - NE_0. \quad (52)$$

For the surfaces studied in this paper the total energies were calculated using the expression

$$E_{\text{tot}} = \sum_{\vec{k}} E_n(\vec{k}) + U_0 N_{\text{bonds}} + \sum_i (U_1 \epsilon_i + U_2 \epsilon_i^2) \quad (53)$$

discussed in Sec. VI A. The surface energy per unit area γ defined as¹⁶

$$\gamma = E_{\text{surf}} \quad (54)$$

(per unit area) is a very useful index for comparing surfaces with different atoms per unit cell and with different periodicities. The calculated surface energies per unit area for several surfaces are discussed in Secs. III–V.

C. Hellmann-Feynman forces

The calculations of Hellmann-Feynman forces within the tight-binding scheme can be done easily. A knowledge of the spatial character of the s and p basis functions used in the calculations is *not* required. In fact, only the expansion coefficients $\lambda_{m,n}$ of the eigenfunctions

$$\psi = \sum_{m,n} \lambda_{m,n} f_m(\vec{r} - \vec{\tau}_n) \quad (55)$$

in terms of the basis functions f_m are needed. In Eq. (55) f_m represents s , p_x , p_y , and p_z functions and τ_n denotes atomic positions. The force on atom i arising from the first term of E_{tot} in Eq. (53) is given by

$$\vec{F}_n = - \sum_j \left\langle \psi_j \left| \frac{\partial H}{\partial \tau_n} \right| \psi_j \right\rangle, \quad (56)$$

where the sum j is over occupied levels E_j with eigenfunction ψ_j . For periodic systems, the sum over j is replaced by sums over the band index and wave vector. Since the tight-binding matrix elements are analytic functions of the atomic coordinates, the gradients $\partial H / \partial \tau_n$ can be easily evaluated. The calculation of \vec{F}_n involves a sum of the form

$$\sum_{m,m',n'} \lambda_{m,n}^* \lambda_{m',n'} \frac{\partial H_{m'n',mn}}{\partial \tau_n} \quad (57)$$

where $H_{m'n',mn}$ is the hopping matrix element between basis functions f_m and $f_{m'}$ localized at sites τ_n and $\tau_{n'}$, respectively. The d^{-2} dependence of the tight-binding matrix elements on distance as well as the gradients of the $(U_1 \epsilon + U_2 \epsilon^2)$ components of the total energy are also easily taken into account in calculating the total force on each atom. The optimal atomic coordinates for each structure can be determined by an iterative process in which atoms are displaced by an amount proportional to the forces acting on them and the new wave functions are calculated. The use of Hellmann-Feynman forces simplifies enormously the determination of complex structures with many degrees of freedom. The relaxed and reconstructed geometries examined in this paper were all determined via a minimization of Hellmann-Feynman forces.

The force acting on an atom can sometimes vanish as a result of symmetry (e.g., when the structure has inversion or mirror-reflection symmetry). In such cases it is often necessary to break the symmetry to find whether the resulting forces restore the symmetry or lead to a new equilibrium configuration. Two examples of structures with broken mirror symmetries at the surface are the asymmetric dimer model²¹ for Si(100) and the dimerized π -bonded chain structure for C(111) surfaces.²⁶

VII. CONCLUSIONS

In conclusion, the surface energies for several structural models of Si(211), Si(311), and Si(331) surfaces were determined. The surface energies of the vicinal surfaces were always found to be higher than for the Si(111)- 2×1 cleavage face even for structures with very low dangling-bond densities. The lower surface energy of the (331) surface, as compared to the (211) surface and the absence of (331)-type steps, i.e., $(11\bar{2})$ propagating steps on cleaved surfaces, indicates the importance of the (111) - 2×1 π -bonded chain reconstruction, occurring in the process of cleavage, in determining the type of step geometry that can occur at the surface.

ACKNOWLEDGMENT

This work is supported in part by the U. S. Office of Naval Research through Contract No. N00014-82-C-0244.

¹R. C. Sangster, in *Compound Semiconductors*, edited by R. K. Willardson and H. L. Goering (Reinhold, London, 1962), Vol. 1, p. 241; in particular, see p. 252.

²G. H. Olsen, T. J. Zamerowski, and F. Z. Hawrylo, *J. Cryst. Growth* **59**, 654 (1982).

³S. L. Wright, M. Inada, and H. Kroemer, *J. Vac. Sci. Technol.* **21**, 534 (1982).

⁴K. C. Pandey, in *Proceedings of the 16th International Conference on the Physics of Semiconductors*, edited by M. Averous (North-Holland, Amsterdam, 1983), p. 761.

⁵B. Z. Olshanetsky and V. I. Mashanov, *Surf. Sci.* **111**, 414

(1981); *Fiz. Tverd. Tela* (Leningrad) **22**, 2923 (1980) [*Sov. Phys.—Solid State* **22**, 1705 (1980)].

⁶B. Z. Olshanetsky and A. A. Shklyayev, *Surf. Sci.* **82**, 445 (1979).

⁷The surface normals are always given with respect to the bulk cubic axes.

⁸The lattice translation vectors are in units of the hexagonal lattice constant $a \approx 3.85$ Å and are specified with respect to the (111) surface coordinate system shown in Fig. 1(a).

⁹M. Henzler, *Surf. Sci.* **36**, 109 (1973); M. Henzler and J. Clabes, *Proceedings of the Second International Conference*

- on Solid Surfaces, (Kyoto, Japan, 1974) [Jpn. J. Appl. Phys. Suppl. 2, Pt. 2, 389 (1974)].
- ¹⁰D. J. Chadi and J. R. Chelikowsky, Phys. Rev. B 24, 4892 (1981).
- ¹¹K. C. Pandey, Phys. Rev. Lett. 47, 1913 (1981); 49, 223 (1982).
- ¹²J. E. Northrup and M. L. Cohen, Phys. Rev. Lett. 49, 1349 (1982); J. Vac. Sci. Technol. 21, 333 (1982).
- ¹³J. E. Rowe, S. B. Christman, and H. Ibach, Phys. Rev. Lett. 34, 874 (1975).
- ¹⁴S. Krueger and W. Mönch, Surf. Sci. 99, 157 (1980).
- ¹⁵R. Kaplan, Surf. Sci. 116, 104 (1982).
- ¹⁶The area of the (111)- 1×1 unit cell is taken as the unit of area in all the following discussions on surface energies.
- ¹⁷This value of γ_{111} does not include spin-polarization effects which reduce γ by $\simeq 0.05$ eV per unit area; J. E. Northrup, J. Ihm, and M. L. Cohen, Phys. Rev. Lett. 47, 1910 (1981).
- ¹⁸Y. Chabal, J. E. Rowe, S. B. Christman, and D. A. Zwemer, Phys. Rev. B 24, 3303 (1981).
- ¹⁹D. M. Zehner, C. W. White, and G. W. Ownby, Surf. Sci. 92, L67 (1980).
- ²⁰D. J. Chadi, Phys. Rev. B 19, 2074 (1979); Phys. Rev. Lett. 41, 1062 (1978).
- ²¹D. J. Chadi, J. Vac. Sci. Technol. 16, 1290 (1979); Phys. Rev. Lett. 43, 43 (1979).
- ²²D. Vanderbilt and J. D. Joannopoulos, Phys. Rev. B 22, 2927 (1980).
- ²³R. Del Sole and D. J. Chadi, Phys. Rev. B 24, 7431 (1981).
- ²⁴The value of $U_C = 1.15$ eV is assumed here to be independent of whether the atom is neutral or negatively charged.
- ²⁵M. T. Yin and M. L. Cohen, Phys. Rev. B 24, 2303 (1981).
- ²⁶K. C. Pandey, Phys. Rev. B 25, 4338 (1982).